Resveratrol Attenuates Obesity-Associated Peripheral and Central Inflammation and Improves Memory Deficit in Mice Fed a High-Fat Diet

Byeong Tak Jeon, Eun Ae Jeong, Hyun Joo Shin, Younghyurk Lee, Dong Hoon Lee, Hyun Joon Kim, Sang Soo Kang, Gyeong Jae Cho, Wan Sung Choi, and Gu Seob Roh

Obesity-induced diabetes is associated with chronic inflammation and is considered a risk factor for neurodegeneration. We tested the hypothesis that an AMP-activated protein kinase activator, resveratrol (RES), which is known to exert potent anti-inflammatory effects, would attenuate peripheral and central inflammation and improve memory deficit in mice fed a high-fat diet (HFD). C57BL/6J mice were fed an HFD or an HFD supplemented with RES for 20 weeks. Metabolic parameters in serum were evaluated, and Western blot analysis and immunohistochemistry in peripheral organs and brain were completed. We used the Morris water maze test to study the role of RES on memory function in HFD-treated mice. RES treatment reduced hepatic steatosis, macrophage infiltration, and insulin resistance in HFD-fed mice. In the hippocampus of HFD-fed mice, the protein levels of tumor necrosis factor-α and Iba-1 expression were reduced by RES treatment. Choline acetyltransferase was increased, and the phosphorylation of tau was decreased in the hippocampus of HFD-fed mice upon RES treatment. In particular, we found that RES significantly improved memory deficit in HFD-fed mice. These findings indicate that RES reverses obesity-related peripheral and central inflammation and metabolic derangements and improves memory deficit in HFD-fed diabetic mice. ***Diabetes*** **61:1444–1454, 2012**

Obesity is a major risk factor for the development of insulin resistance, type 2 diabetes, stroke (1), and Alzheimer disease (AD) (2). It is well established that obesity is characterized by abnormal adipokine production and activation of some proinflammatory signaling pathways (3,4). Chronic inflammation associated with obesity is also characterized by macrophage infiltration into adipose tissues (5). Insulin resistance in peripheral tissues could influence central insulin resistance with reduced brain insulin levels (6). Therefore, peripheral insulin resistance could affect cognition (7). A number of epidemiological studies provide direct evidence to strengthen the link between type 2 diabetes and AD (8). The progressive worsening of insulin resistance with AD is correlated with increased oxidative stress, lipid peroxidation manifested by 4-hydroxynonenal (4-HNE), and inflammation (9). A recent study demonstrates that resveratrol (RES), a polyphenolic compound enriched in grapes and red wine, prevents memory deficits and the increase in acetylcholinesterase activity in streptozotocin (STZ)-induced diabetic rats (10).

RES has attracted wide attention because of its antioxidant and anti-inflammatory effects (11). Recent evidence shows that treatment with RES ameliorates elevated levels of tumor necrosis factor (TNF)-α, interleukin (IL)-6, and cyclooxygenase-2 in experimental diabetic neuropathy (12). AICAR, an activator of AMP-activated protein kinase (AMPK), has been reported to show anti-inflammatory and immunomodulatory effects in experimental autoimmune encephalomyelitis or lipopolysaccharide (LPS)-stimulated rats (13,14). RES has also been demonstrated to promote degradation of amyloid-β (A-β) peptide in AD (15).

RES increases AMPK activity and improves insulin sensitivity (16). AMPK is an energy sensor that regulates energy homeostasis and metabolic stress (17). By affecting glucose and lipid metabolism, energy balance is closely related to obesity and type 2 diabetes. The activation of AMPK is responsible for metabolic changes via phosphorylation of downstream substrates, such as acetyl CoA carboxylase (ACC) and glycogen synthase kinase (GSK)-3β, which are directly related to glycogen synthesis and fatty acid oxidation, respectively (18,19). In particular, data from AMPK-deficiency models suggest that AMPK activity might influence the pathophysiology and therapy of diabetes (17). Interactions between insulin and the AMPK signaling pathway were reported in liver, skeletal muscle, and adipocytes (19). In the central nervous system (CNS), it has been demonstrated that the ability of leptin to modulate both tau-phosphorylation and A-β production is mediated through AMPK (20).

Although many studies show neuroprotective effects of RES in STZ-administered rodents, the effects of RES on the hippocampus in obesity-induced diabetes are not fully known. Therefore, the purpose of the current study was to determine whether chronic, dietary RES administration not only enhances insulin resistance and peripheral inflammation but also prevents neuroinflammation and memory deficits in mice fed a high-fat diet (HFD). Our findings suggest that obesity- or diabetes-related systemic inflammation, neuroinflammation, and memory deficits in type 2 diabetic mice can be prevented or delayed by RES supplementation.

RESEARCH DESIGN AND METHODS

Animals and obesity model. Male C67BL/6J mice (3 weeks old) were purchased from KOATECH (Pyeongtaek, South Korea) and maintained in the animal facility at Gyeongsang National University. The experiments were performed in accordance with the National Institutes of Health Guidelines on the Use of Laboratory Animals. The university animal care committee for animal research of Gyeongsang National University approved the study protocol (GLA-101104-M0108). Mice were individually housed with an alternating 12-h light/dark cycle. Mice, starting at age 4 weeks, were randomly divided into

From the Department of Anatomy and Neurobiology, Institute of Health Sciences, Medical Research Center for Neural Dysfunction, Gyeongsang National University School of Medicine, Jinju, Gyeongnam, Republic of Korea.
Corresponding author: Gu Seob Roh, anaroh@gnu.ac.kr.
Received 25 October 2011 and accepted 18 December 2011.
DOI: 10.2337/db11-1498

four groups (n = 30 per group). Mice were fed for 20 weeks with either HFD (60%) or low-fat diet (LFD, 10%) chow (Research Diets, Inc., New Brunswick, NJ). Mice were dosed with 200 mg/kg of *trans*-RES (ChromaDex, Inc., Irvine, CA) daily in either LFD or HFD chow. Mice were weighed four times weekly and just prior to killing at age 24 weeks.

Glucose tolerance test. Mice were fasted overnight (16 h) before a glucose tolerance test (GTT). D-glucose (2 g/kg; Sigma-Aldrich, St. Louis, MO) was injected intraperitoneally, and blood samples were taken before and 30, 60, 90, and 120 min after the injection of glucose. Blood glucose was measured using an Accu-Chek glucometer (Roche Diagnostics GmbH, Mannheim, Germany).

Insulin tolerance test. The insulin tolerance test (ITT) was performed on mice at approximately 2:00 P.M. Mice were injected with insulin (0.75 units/kg; Humulin-R; Eli Lilly and Company, Indianapolis, IN) in 0.1 mL 0.9% normal saline. A drop of blood was taken from the cut tail vein before and 15, 30, 45, and 60 min after the injection of insulin for the determination of blood glucose with a glucometer (Accu-Chek).

Enzyme-linked immunosorbent assay. Serum adiponectin, leptin, insulin, and TNF-α concentrations (n = 5–6 per group) were measured using adiponectin, leptin, and insulin mouse ELISA kits (Alpco Diagnostics, Salem, NH) and a mouse TNF-α ELISA kit (BD, Franklin Lakes, NJ) according to the manufacturers' protocols.

Tissue collection and sample preparations. For tissue analysis, mice (n = 7 per group) were anesthetized with zoletil (5 mg/kg, Virbac Laboratories, Carros, France) and then perfused transcardially with heparinized saline followed by 4% paraformaldehyde in 0.1 mol/L PBS. Six hours after postfixation in the same fixative, the brains were sequentially immersed in 0.1 mol/L PBS containing 15% sucrose and then in PBS containing 30% sucrose at 4°C until they sank. The brains were cut into 40 μm–thick coronal sections. Other tissues, including liver, epididymal fat pads, and pancreas, were processed for paraffin embedding and sectioned (5 μm).

Oil Red O staining. Oil Red O staining is commonly used to identify lipid deposits. To determine hepatic lipid accumulation, frozen sections (5 μm) of liver were stained with 0.5% Oil Red O (Sigma-Aldrich) for 10 min, washed, and counterstained with Mayer's hematoxylin (Sigma-Aldrich) for 45 s. The sections were visualized under a BX51 light microscopy (Olympus, Tokyo, Japan), and digital images were captured and documented.

Rapid Golgi staining. For rapid Golgi staining, mice (n = 3 per group) were intraperitoneally anesthetized with 5 mg/kg zoletil (Virbac Laboratories) and brains were removed from the skull as quickly as possible and rinsed briefly in distilled water. Golgi staining was performed with an FD rapid GolgiStain kit (PK 401; FD NeuroTechnologies, Inc., Ellicott City, MD) according to the manufacturer's protocol. Coronal sections (150 μm) of Golgi-stained brains were cut with a slicetome (Meiwa Shoji Co., Osaka, Japan). Slices were mounted on microscope slides (Fisherbrand; Fisher Scientific, Waltham, MA). The sections were visualized under a BX51 light microscopy (Olympus).

Immunohistochemistry. Deparaffinized sections from liver, pancreas, and epididymal fat pads or frozen sections from brains were placed in a solution of 0.3% H_2O_2 for 10 min. After washing, sections were treated with diluted blocking serum for 20 min. Slides were incubated overnight at 4°C in a humidified chamber with anti–mouse-4-HNE (1:100; Abcam, Cambridge, MA), anti–rabbit-F4/80 (1:100; Santa Cruz Biotechnology, Santa Cruz, CA), anti–rabbit-CD68 (1:100; Santa Cruz Biotechnology), and anti–guinea pig-insulin (1:100; Abcam) diluted in blocking serum. After washing three times with 0.1 mol/L PBS, sections were incubated for 1 h at room temperature with a secondary biotinylated antibody (1:200). After washing, sections were incubated in avidin-biotin-peroxidase complex solution (Vector Laboratories, Burlingame, CA). Sections were developed with 0.05% diaminobenzidine (Sigma-Aldrich) containing 0.05% H_2O_2 and were dehydrated through graded alcohols, cleared in xylene, and coverslipped with Permount (Sigma-Aldrich). Sections were visualized under a BX51 light microscopy (Olympus). Photomicrographs were assessed by densitometry using the analySIS FIVE program (Olympus Soft Imaging Solutions, Münster, Germany). For immunostaining for Iba-1 (1:200; Wako Pure Chemical Industries, Osaka, Japan) and choline acetyltransferase (ChAT; 1:100; Millipore, Billerica, MA), free-floating sections were labeled with Iba-1 antibody overnight at 4°C. Sections were incubated with Alexa Fluor 594–conjugated donkey anti-rabbit antibody (1:1,000; Invitrogen, Carlsbad, CA). Fluorescence was visualized under a confocal microscope (FV-1000; Olympus).

Western blot analysis. For protein extraction, frozen hippocampi were homogenized in a lysis buffer. The following antibodies were used: TNF-α (Santa Cruz Biotechnology); Iba-1 (Wako Pure Chemical Industries); p–insulin receptor (IR) and IR (both from Millipore); p-AMPK, AMPK, p-ACC, ACC, p–GSK-3β, and GSK-3β (all from Cell Signaling Technology, Danvers, MA); and p-tau, tau, ChAT, and 4-HNE (all from Santa Cruz Biotechnology). The membranes were probed with each antibody or α-tubulin (Sigma-Aldrich) and visualized using an enhanced chemiluminescence substrate (Pierce, Rockford, IL). The Multi-Gauge version 3.0 image analysis program (Fujifilm, Tokyo, Japan) was used to measure band densitometry.

Morris water maze test. Morris water maze testing was performed as previously described (21), with the following modifications. In brief, mice (n = 10 per group) were first trained to find a randomly positioned visible platform in a 100 cm–diameter swimming pool, maintained at 25.0 ± 1°C. All mice were subjected to four trials per day for 4 consecutive days. The escape latency and swimming distance to find the platform was recorded by a video-tracking program (Noldus EthoVision XT7; Noldus Information Technology, Wageningen, the Netherlands). On the day of testing, the platform was removed and time spent in the target quadrant, where the platform had been located during training, was analyzed. The starting position was changed with each trial.

Statistics. Differences between mice fed an LFD, HFD, HFD plus RES, or LFD plus RES were determined by two-way ANOVA, followed by Bonferroni post hoc analysis. Values are expressed as the mean ± SEM. $P < 0.05$ was considered statistically significant.

RESULTS

RES does not reduce the body weight of HFD-fed mice. Mice were fed an HFD for 20 weeks. After 2 weeks, the body weight gradually increased in HFD-fed mice compared with LFD-fed mice (Fig. 1*A*). However, RES did not cause any reduction in body weight in HFD-fed mice. Next, whole brain weights were measured at the time of killing. Although brain weights were unchanged (data not shown), the ratio of brain to body weight was significantly decreased in HFD-fed mice compared with LFD-fed mice (Fig. 1*B*). However, the ratio was not changed by RES treatment.

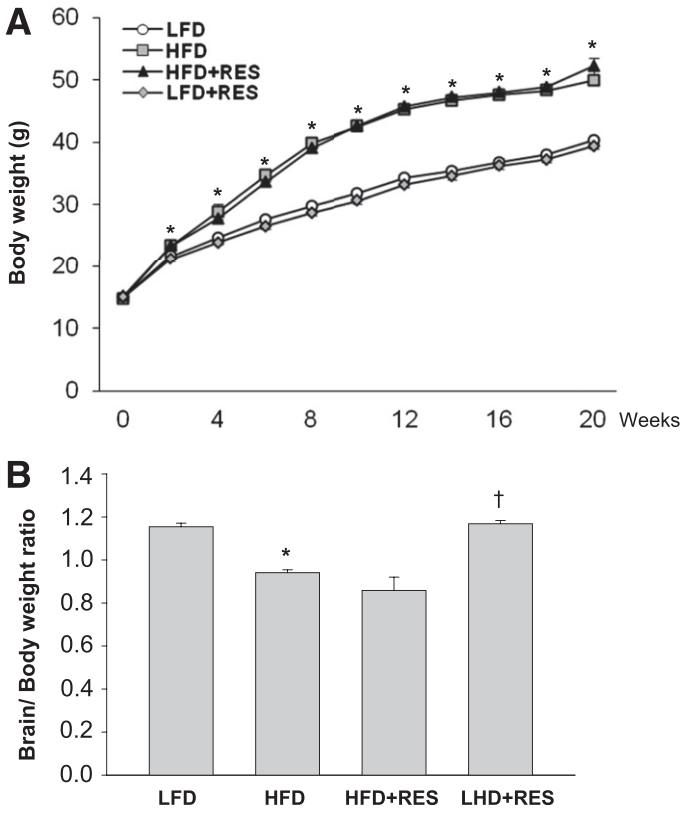

FIG. 1. Effects of RES on whole body and brain weight in HFD-fed mice. Male C57BL/6J mice were fed an LFD, HFD, HFD+RES, or LFD+RES for 20 weeks (n = 20 per group). *trans*-RES was homogenously blended into the LFD or HFD, pelleted, and preserved in a manner to ensure the stability of RES. Graphs show change in body weight (*A*) and ratio of brain to body weight (*B*) for each group at time of killing (age 24 weeks). Data are mean ± SEM. *P < 0.005 for HFD- compared with LFD-fed mice. †P < 0.001 for mice fed an LFD+RES compared with HFD-fed mice.

RES improves insulin sensitivity in HFD-fed mice. To determine the effects of RES on serum adipokines in the LFD- and HFD-fed mice, we measured the concentration of adiponectin and leptin using enzyme-linked immunosorbent assay (ELISA) (Fig. 2*A* and *B*). HFD-induced hypoadiponectinemia and hyperleptinemia were significantly reversed by RES treatment. Next, to explore the role of RES in obesity-induced insulin resistance, GTTs and ITTs were performed (Fig. 2*C* and *D*). HFD-fed mice were significantly more glucose tolerant after a 20-week HFD challenge (Fig. 2*C*); however, administration of RES reduced glucose tolerance 30 min after intraperitoneal injection of glucose in HFD-fed mice. Consistent with the effects of RES on GTTs, the reduction in glucose levels during ITTs

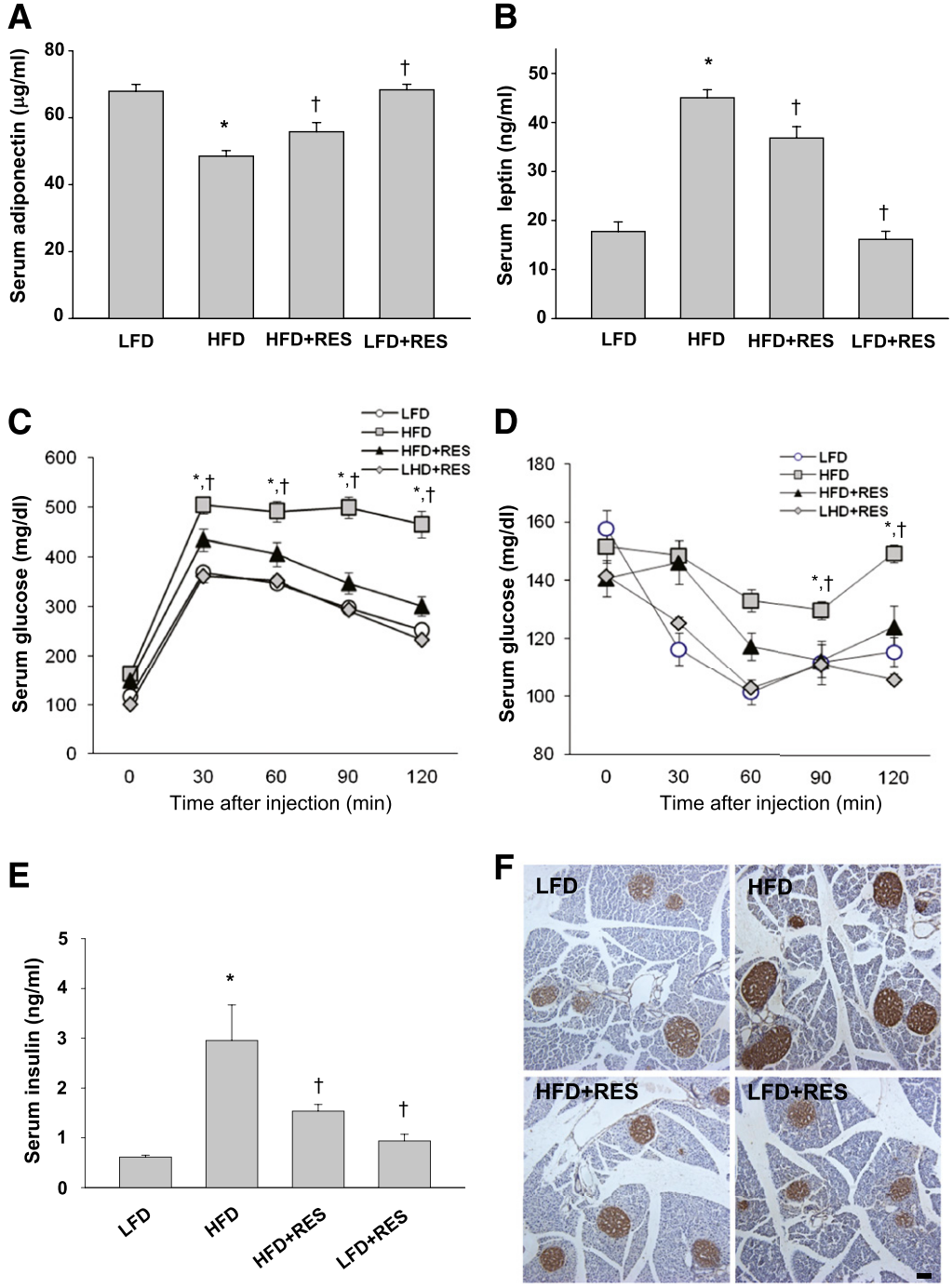

FIG. 2. Effects of RES on metabolic parameters in HFD-fed mice. For ELISA analysis, mice were anesthetized with zoletil (5 mg/kg) and then blood serum was extracted transcardially through the apex of the left ventricle with a 1-mL syringe. Serum adiponectin (*A*) and leptin (*B*) levels using ELISA (n = 5–7 per group). Hypoadiponectinemia and hyperleptinemia in HFD-fed mice were significantly reversed by RES treatment. *C*: Blood glucose levels after D-glucose (2 g/kg) injection in mice fed an LFD, HFD, HFD+RES, or LFD+RES. *D*: Blood glucose levels after insulin treatment (0.75 units/kg). Blood glucose levels of mice fed an HFD+RES were significantly decreased compared with HFD-fed mice. *E*: Serum insulin (n = 5–7 per group) levels using ELISA. RES decreased HFD-induced hyperinsulinemia. *F*: Representative microphotographs of immunostained insulin in pancreatic sections from mice fed an LFD, HFD, HFD+RES, or LFD+RES. Data are mean ± SEM. *P < 0.05 for HFD- compared with LFD-fed mice. †P < 0.05 for mice fed an LFD or HFD+RES compared with HFD-fed mice. Scale bar = 100 μm. (A high-quality color representation of this figure is available in the online issue.)

was greater in mice fed an HFD plus RES (Fig. 2*D*). Hyperinsulinemia in HFD-fed mice was significantly reduced by RES treatment (Fig. 2*E*). Finally, to examine islet morphology and production of insulin, immunostaining for insulin was performed on pancreas sections from each group of mice (Fig. 2*F*). Although there was no difference in the diameter of pancreatic islets between the groups, the relative densities (10.48 ± 1.52) of immunostained insulin-positive cells in the pancreatic islets of HFD-fed mice were higher (1.0 ± 0.34) than that of LFD-fed mice ($P < 0.001$). However, the relative density (0.99 ± 0.20) in HFD-fed mice was significantly reduced by RES treatment ($P < 0.001$).

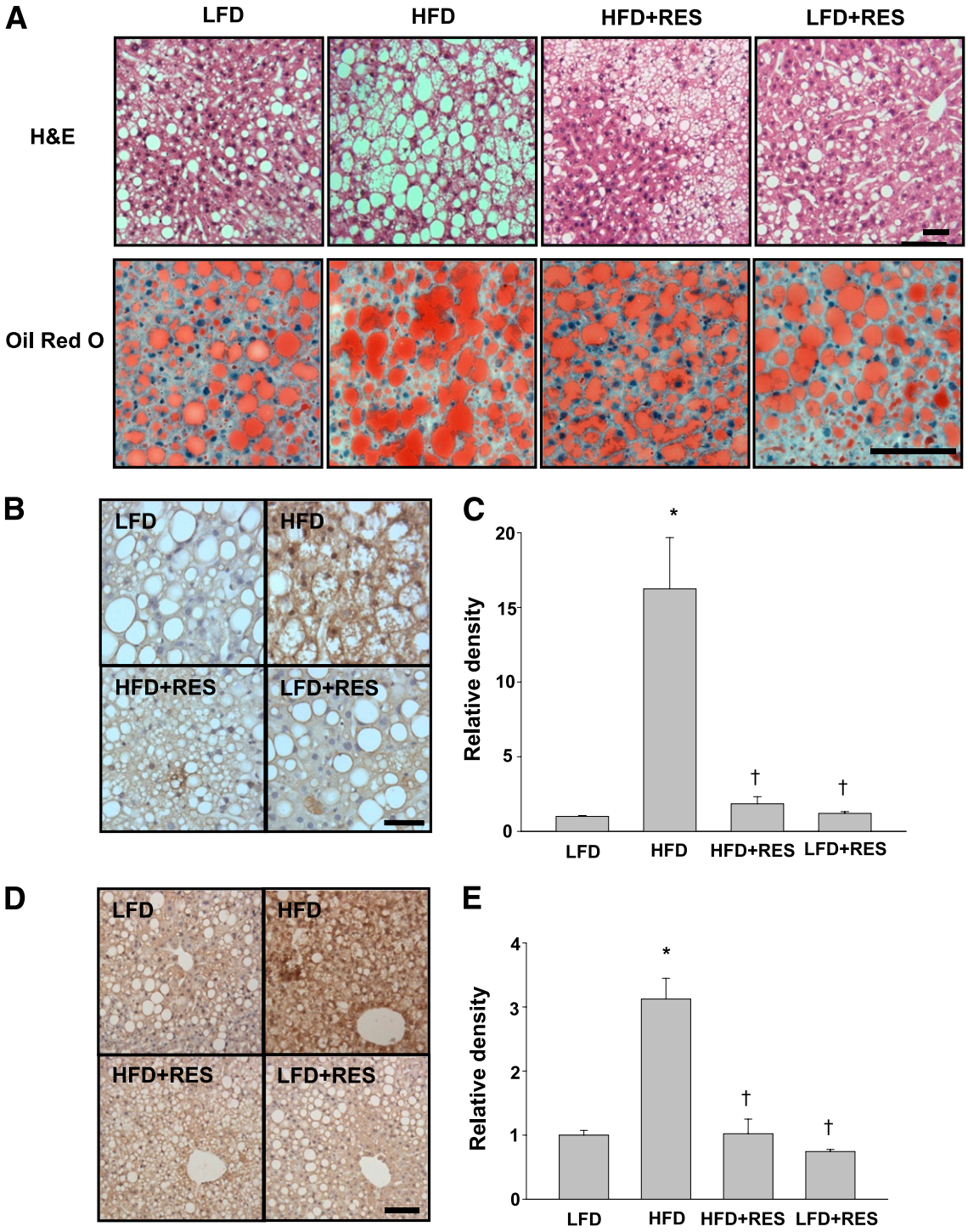

FIG. 3. Effects of RES on hepatic steatosis, oxidative stress, and macrophage infiltration in HFD-fed mice. *A*: Representative microphotographs of hematoxylin and eosin (H&E)- and Oil Red O–stained liver section from mice fed an LFD, HFD, HFD+RES, or LFD+RES. *B*: Representative microphotographs of immunostained 4-HNE in liver sections from each group. *C*: Quantitative expression of 4-HNE is shown as relative density. *D*: Representative microphotographs of immunostained F4/80 in liver sections from each group. *E*: Quantitative expression of F4/80 is shown as relative density. Data are mean ± SEM. *$P < 0.05$ for HFD- compared with LFD-fed mice. †$P < 0.05$ for mice fed an LFD or HFD+RES compared with HFD-fed mice. Scale bar = 50 μm. (A high-quality digital representation of this figure is available in the online issue.)

RES reduces hepatic steatosis, lipid peroxidation, and macrophage infiltration in HFD-fed mice. Hepatic steatosis as fatty liver disease is characterized by the accumulation of fats, oxidative stress–induced lipid peroxidation, and macrophage infiltration (22). To examine the effects of RES on hepatic steatosis, we performed hematoxylin and eosin and Oil Red O staining (Fig. 3*A*). Histologic examination showed that hepatocytes of HFD-fed mice were distended by large cytoplasmic lipid droplets. This change in cellular morphology was prevented by RES treatment (Fig. 3*A*). Next, we confirmed the effect of RES on lipid peroxidation in the liver of HFD-fed mice using immunohistochemistry for 4-HNE (Fig. 3*B*). There were significant increases in immune densities in HFD-fed mice compared with LFD-fed mice, which were reduced by RES treatment (Fig. 3*C*). Finally, we found that immunostaining for F4/80, a macrophage marker, in HFD-fed mice was also significantly reduced by RES treatment (Fig. 3*D* and *E*).

RES reduces serum TNF-α and macrophage infiltration of adipose tissue in HFD-fed mice. We measured serum concentration of TNF-α levels using ELISA (Fig. 4*A*). The circulation levels of TNF-α were significantly increased in HFD-fed mice compared with LFD-fed mice ($P = 0.046$). However, this HFD-induced increase in TNF-α was attenuated by RES treatment ($P = 0.023$). To investigate the effect of RES on macrophage accumulation in HFD-fed mouse epididymal fat pads, we performed immunohistochemistry with anti-CD68 antibody (Fig. 4*B*). Figure 4*B* shows that many CD68-expressing cells were deposited in the adipose tissue of HFD-fed mice. In accordance with the role of RES on serum TNF-α, RES reduced immune density of CD68 in epididymal fat pads of HFD-fed mice (Fig. 4*C*).

RES attenuates neuroinflammation and oxidative stress in the hippocampus of HFD-fed mice. In addition to peripheral tissues, obesity is associated with an increased risk for dementia and neuroinflammation (23). Among brain regions, the hippocampus is particularly vulnerable in AD (24). Western blot analysis showed that HFD-induced TNF-α and Iba-1 expression was significantly decreased by RES treatment (Fig. 5*A* and *B*). Immunohistochemical analysis showed activated microglia in the hippocampus of HFD-fed mice (Fig. 5*C*). However, there were many ramified, resting microglia in the hippocampus of mice fed an LFD or HFD plus RES. We also evaluated the effect of RES

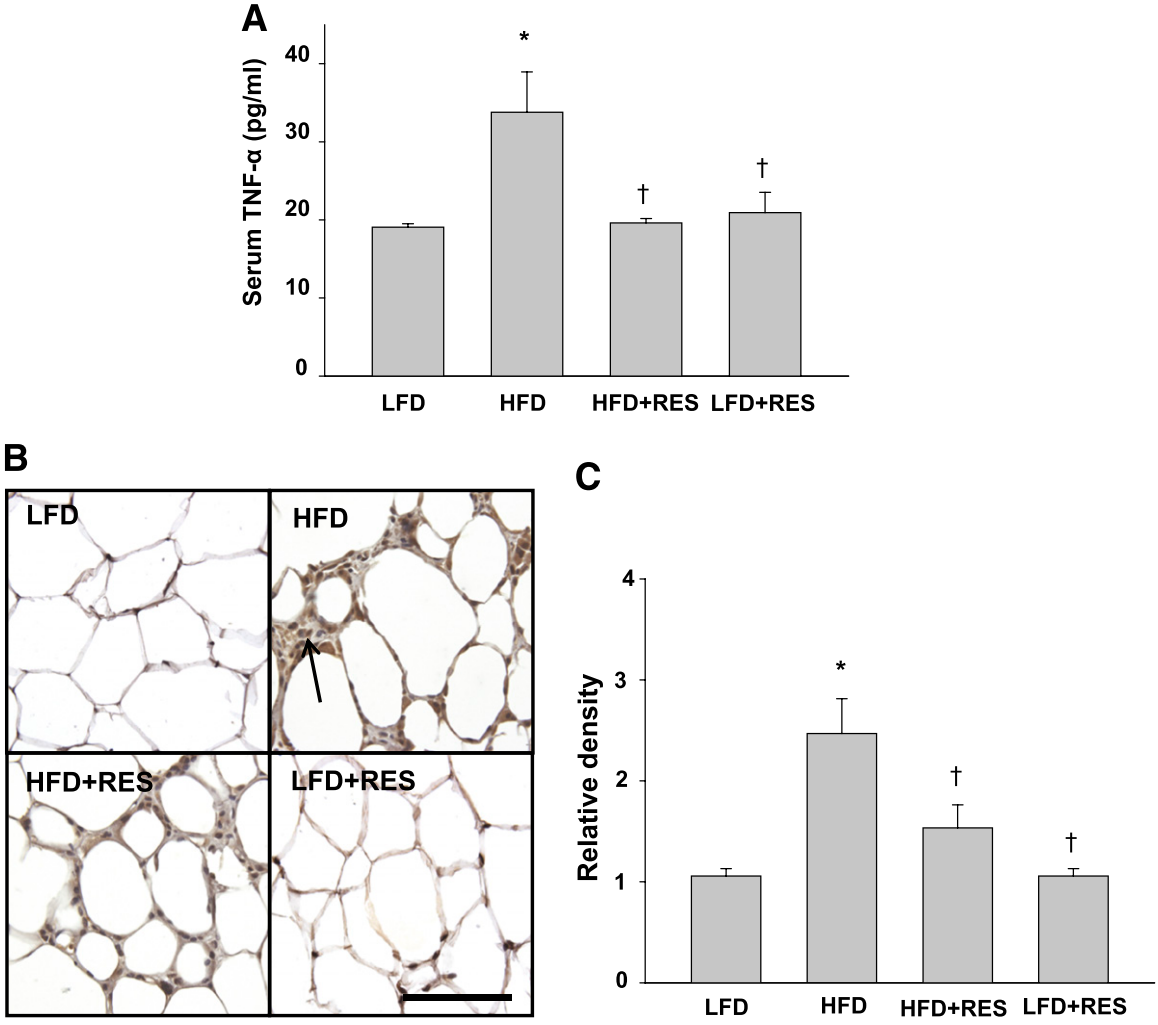

FIG. 4. Effects of RES on serum TNF-α and macrophage infiltration in adipose tissue in HFD-fed mice. *A*: Concentration of TNF-α (n = 5–7 per group) from serum of mice fed an LFD, HFD, HFD+RES, or LFD+RES using ELISA. RES significantly inhibited the HFD-induced increase of TNF-α production. *B*: Representative microphotographs of immunostained CD68 in epididymal fat pads from each group. CD68-expressing cells were deposited in HFD-treated adipose tissue. Arrow indicates macrophage. Scale bar = 50 μm. *C*: Quantitative expression of CD68 is shown as relative density. Data are mean ± SEM. *$P < 0.05$ for HFD- compared with LFD-fed mice. †$P < 0.05$ for mice fed an LFD or HFD+RES compared with HFD-fed mice. (A high-quality color representation of this figure is available in the online issue.)

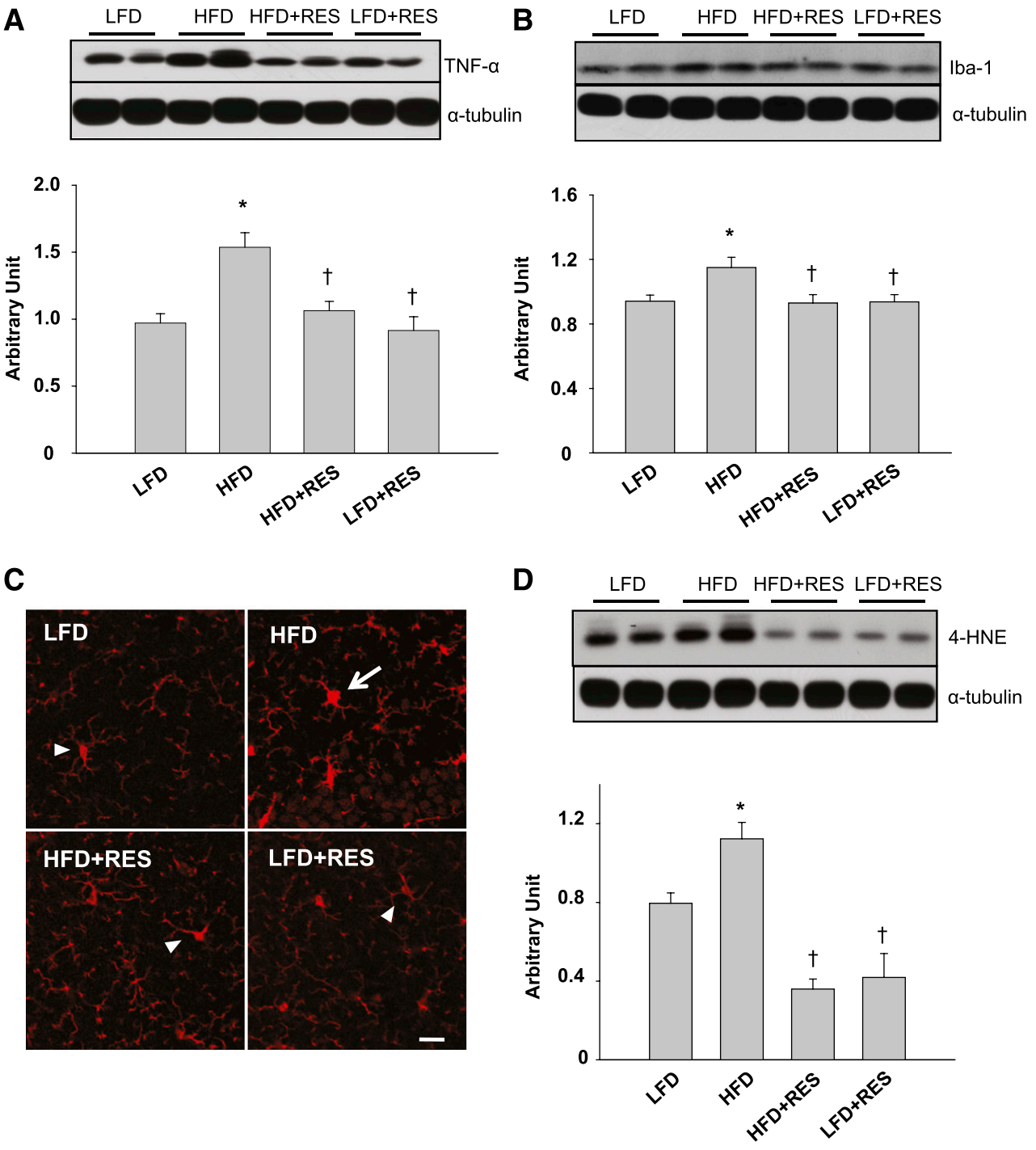

FIG. 5. Effects of RES on neuroinflammation in the hippocampus of HFD-fed mice. *A*: Western blot showing hippocampal TNF-α in mice fed an LFD, HFD, HFD+RES, or LFD+RES. Quantification of hippocampal TNF-α from Western blot analysis. Densitometry values for TNF-α were normalized to α-tubulin and are represented as arbitrary units (AUs). *B*: Western blot showing hippocampal Iba-1 in each group of mice. Quantification of hippocampal Iba-1 from Western blot analysis. Densitometry values for Iba-1 were normalized to α-tubulin and are represented as AUs. *C*: Representative microphotographs of immunostained Iba-1 in CA1 region of the hippocampus from each group. Ramified microglia are present in the hippocampus of mice fed an LFD, HFD+RES, or LFD+RES, whereas activated microglia are present in HFD-fed mice. Arrow or arrowheads indicate activated microglia or ramified microglia, respectively. Scale bar = 20 μm. *D*: Western blot showing hippocampal 4-HNE in each group of mice. Quantification of hippocampal 4-HNE from Western blot analysis. Densitometry values for 4-HNE were normalized to α-tubulin and are represented as AUs. Data are mean ± SEM. *$P < 0.05$ for HFD- compared with LFD-fed mice. †$P < 0.05$ for mice fed an LFD or HFD+RES compared with HFD-fed mice. (A high-quality color representation of this figure is available in the online issue.)

on lipid peroxidation in the hippocampus of HFD-fed mice (Fig. 5*D*). Western blot analysis revealed that HFD resulted in increased hippocampal 4-HNE expression compared with LFD-fed mice. However, RES significantly attenuated this HFD-induced increased expression of 4-HNE. It is interesting that there was also a significant decrease in 4-HNE expression in mice fed an LFD plus RES.

RES improves insulin resistance and energy metabolism in the hippocampus of HFD-fed mice. Hyperphosphorylation of tau-protein is potentiated by a disturbance of glucose

and energy metabolism (25). In Western blot analysis with anti–p-IR and total IR antibodies, the expression levels of p-IR were significantly decreased in HFD-fed mice compared with LFD-fed mice, whereas the ratio of p-IR to IR protein expression was increased by RES treatment (Fig. 6*A*). In accordance with serum adiponectin levels, the decreased hippocampal expression of adiponectin in the HFD-fed mice was increased by RES (Fig. 6*B*). Next, we evaluated the effects of RES on the adiponectin-mediated AMPK signaling pathway in HFD-fed mice (Fig. 6*C* and *D*). Western blot analysis showed that levels of hippocampal p-AMPK and p-ACC were significantly decreased in the HFD-fed mice compared with LFD-fed mice. However, RES increased the phosphorylation of p-AMPK and p-ACC in HFD-fed mice. Finally, to test whether RES affects AMPK-mediated phosphorylation of GSK-3β and tau in the hippocampus of HFD-fed mice, we performed Western blot analysis (Fig. 6*E* and *F*). Mice fed an HFD plus RES showed neither an HFD-induced decrease in the ratio of p–GSK-3β to GSK-3β nor an increase in the ratio of p-tau to tau in the hippocampus.

RES inhibits neurodegeneration in the hippocampus of HFD-fed mice. Golgi staining has been commonly used for neuronal morphometry in neurodegenerative disorders (26). In serial coronal sections of the hippocampus (Fig. 7*A*), we found that neurons from HFD-fed mice showed less dendritic branching and decreased branch length and complexity of neuronal dendritic trees compared with mice fed an HFD plus RES (Fig. 7*B*).

RES enhances cognitive function in HFD-fed mice. We evaluated the effect of RES on hippocampal ChAT expression in HFD-fed mice using Western blot analysis and immunohistochemistry (Fig. 8*A* and *B*). Western blot analysis showed that hippocampal ChAT expression in HFD-fed mice was decreased compared with LFD-fed mice, and RES attenuated this HFD-induced effect (Fig. 8*A*). In immunohistochemical analysis, ChAT-positive cells were distributed in the neurites of neurons in the CA1 region in the hippocampus of mice fed an LFD or HFD plus RES (Fig. 8*B*). However, ChAT-immunoreactive positive neurons and neurites had comparatively the least immunoreactivity in the HFD-treated mice. Finally, to assess whether RES affects memory deficits in HFD-induced obesity, we performed the Morris water maze test after 20 weeks of HFD administration (Fig. 8*C–F*). HFD-fed mice exhibited increased escape latencies and swimming distance (Fig. 8*C* and *D*) during training trials and reduced time spent in target quadrant during Morris water maze testing (Fig. 8*E*), whereas RES treatment significantly decreased escape latency and

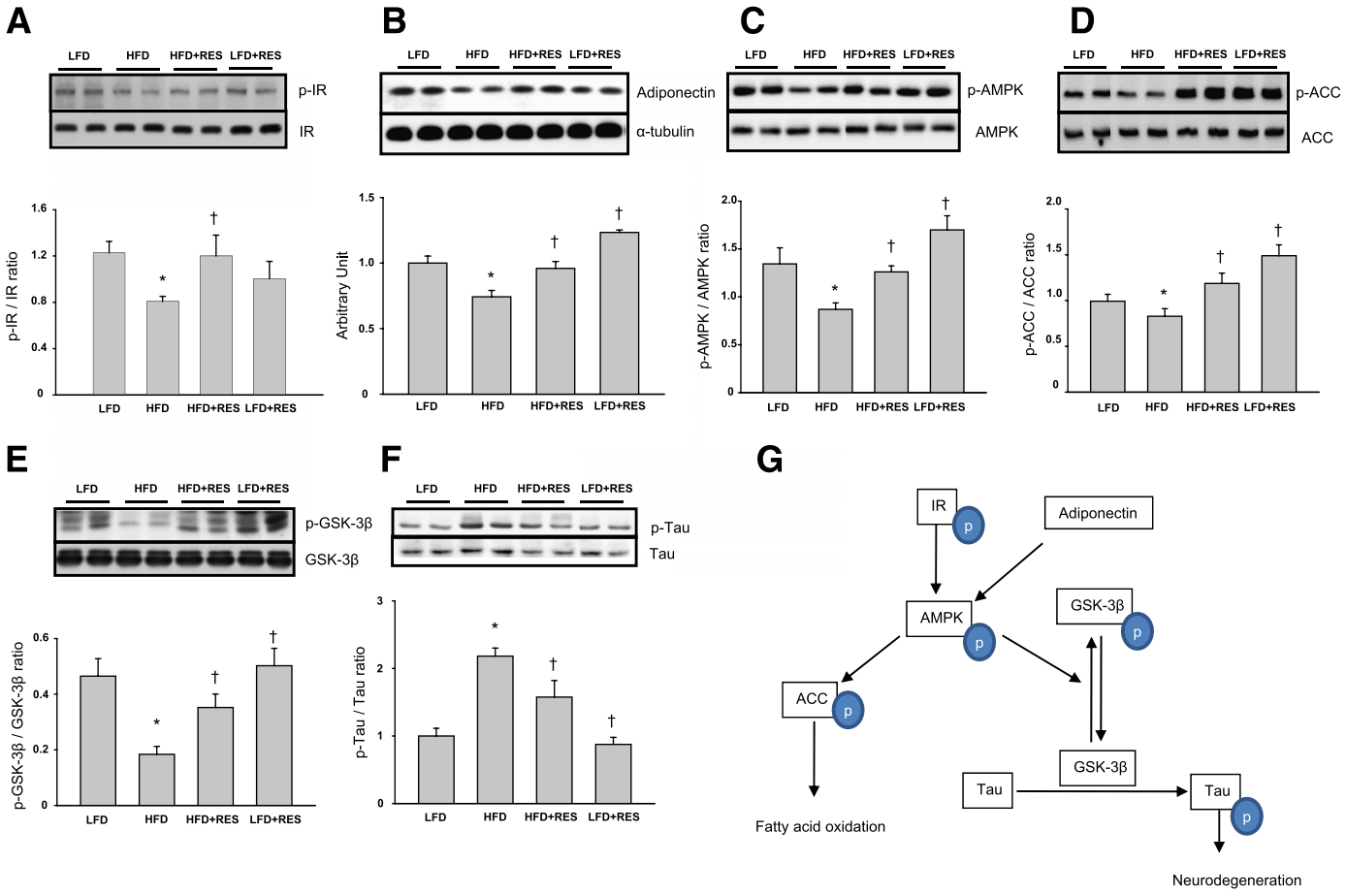

FIG. 6. Effects of RES on IR-mediated AMPK signaling pathway in the hippocampus of HFD-fed mice. *A*: Western blot showing p-IR and IR in the hippocampus of mice fed an LFD, HFD, HFD+RES, or LFD+RES. Densitometry values of p-IR were normalized to IR and represented as arbitrary units (AUs). *B*: Western blot showing adiponectin in the hippocampus. Densitometry values of adiponectin were normalized to α-tubulin and represented as AUs. Western blot showing phosphorylation of AMPK (*C*), ACC (*D*), GSK-3β (*E*), and tau (*F*) in the hippocampus from each group. Quantification of the phosphorylation of each protein from Western blot analysis. Densitometry values for each p-protein were normalized to total protein and are represented as AUs. Data are mean ± SEM. *$P < 0.05$ for HFD- compared with LFD-fed mice. †$P < 0.05$ for mice fed an LFD or HFD+RES compared with HFD-fed mice. *G*: Proposed model of the phosphorylated regulation of IR-mediated AMPK signaling pathway in the hippocampus. (A high-quality color representation of this figure is available in the online issue.)

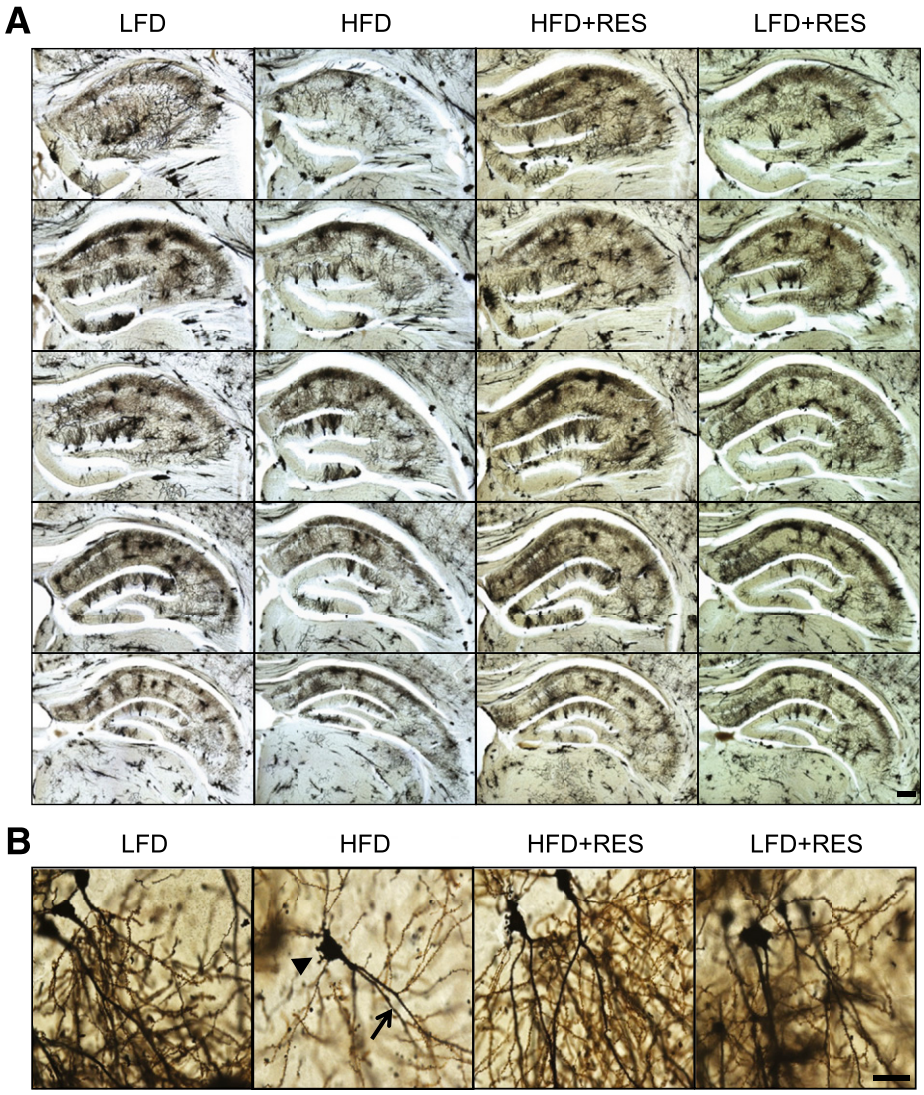

FIG. 7. Effects of RES on neurodegeneration in the hippocampus of HFD-fed mice. *A*: Representative microphotographs of Golgi-stained hippocampus of mice fed an LFD, HFD, HFD+RES, or LFD+RES. Golgi-stained neurons were visualized in the hippocampal regions from bregma −1.22 to −2.54 mm of the mouse brain atlas. *B*: Representative, higher resolution microphotographs of Golgi-stained neurons in the hippocampus of mice fed an LFD, HFD, HFD+RES, or LFD+RES. Arrowhead and arrow indicate neuronal soma and dendrite, respectively. Scale bar = 200 μm (*A*) and 50 μm (*B*). (A high-quality digital representation of this figure is available in the online issue.)

swimming distance and increased time spent in the target quadrant. As shown in Fig. 8*F*, examination of swim paths revealed that HFD-fed mice with RES showed remarkable improvements in spatial bias compared with HFD-fed mice.

DISCUSSION

Previous studies indicate close associations between diabetes-induced chronic inflammation and AD (27). Aged rodents show exaggerated neuroinflammation and memory deficits in response to peripheral inflammation (28). RES has recently received considerable attention because of its antioxidant, anti-inflammatory, and neuroprotective effects, including cognitive deficits associated with type 1 diabetes (10,29). Although some studies have investigated the neuroprotective effects of RES in type 1 diabetes, the actions of RES on the neuronal AMPK pathway and memory in HFD-induced type 2 diabetic mice have not been reported in the literature. In the current study, we found that RES improves not only peripheral inflammation and insulin sensitivity but also neuroinflammation and memory deficit in HFD-fed mice by activation of the AMPK signaling pathway.

RES is known to reduce fat accumulation and improve glucose tolerance and insulin sensitivity in mice with HFD-induced obesity (30). RES reduces body weight through increased mitochondrial biogenesis and physical endurance (31). Um et al. (32) recently demonstrated that RES (400 mg/kg) increases insulin sensitivity and reduces fat mass in 40% HFD-fed mice. In the current study, although RES (200 mg/kg) did improve insulin sensitivity and metabolic parameters in 60% HFD-fed mice, body weight was not reduced by supplementation with RES for 20 weeks. The reasons for this discrepancy are not clear but may be due to differences in the percentage of fat in the respective diets, dose of RES, and duration of diabetes.

There is evidence that a state of chronic, low-grade inflammation is a key link between obesity and the associated metabolic syndrome (33). In general, HFD is a nutritional condition that accounts for the largest incidence of metabolic syndrome in the world (34). Obesity leads to the

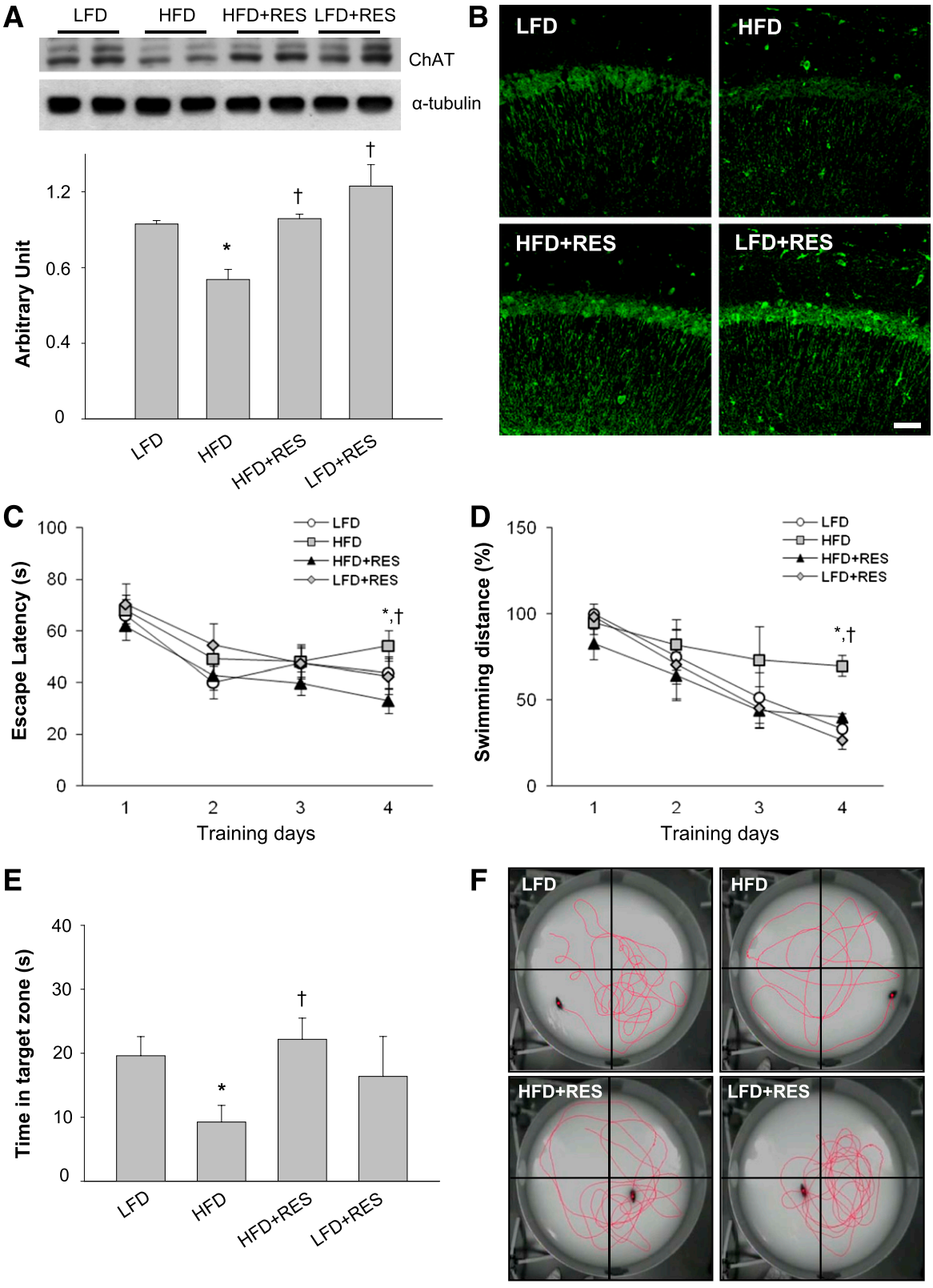

FIG. 8. Effects of RES on hippocampal ChAT expression and memory deficits in HFD-fed mice. *A*: Western blot showing ChAT in the hippocampus. Densitometry values of adiponectin were normalized to α-tubulin and represented as arbitrary units. *B*: Representative microphotographs of immunostained ChAT in CA1 region of the hippocampus from each group. Scale bar = 50 μm. Escape latency (*C*) and swimming distance (*D*) (mean of four trials per day) in the Morris water maze (n = 10 per group) at 24 weeks. *E*: Comparison of time spent in the target quadrant (where the platform was located during hidden-platform training) after removing the exact location of the platform on day 5. Data are mean ± SEM. *$P < 0.05$ for HFD- compared with LFD-fed mice. †$P < 0.05$ for mice fed an LFD or HFD+RES compared with HFD-fed mice. *F*: Representative swim paths in the trial without the platform (probe) in each group. Note that only HFD-fed mice showed a random search pattern, whereas the other groups focused their search around the previous platform location. (A high-quality digital representation of this figure is available in the online issue.)

infiltration of fats into multiple organs, including the epididymis, heart, liver, and pancreas. In particular, macrophages, which infiltrate the adipose tissue of obese rodents and humans, are a major source for proinflammatory cytokines, such as TNF-α and IL-6 (35). Obesity is associated with macrophage accumulation in adipose tissue and increased serum TNF-α, and we found that chronic HFD feeding induced higher circulating levels of TNF-α and macrophage accumulation in epididymal fat pads and liver (Figs. 3 and 4). In addition to these peripheral organs, although there were no significant differences in the levels of IL-6, IL-1β, or TNF-α mRNA in temporal tissues from LFD- and HFD-fed mice (36), we found that HFD feeding increased hippocampal TNF-α expression and activated microglia compared with LFD-fed mice (Fig. 5). In accordance with our result, another study demonstrates that proinflammatory cytokines, such as TNF-α and IL-1β, were released in the hypothalamus and activated apoptotic signaling in the hypothalamus of rodents on an HFD (37). In AD, an abundance of reactive astrocytes and activated microglial cells are found in the proximity of neuritic plaques (38). However, we found no significant difference in glial fibrillary acidic protein expression between LFD- and HFD-fed mice using Western blot and immunohistochemistry (data not shown). The reasons for this finding are not clear but may be due to the dominant response of microglia cells against chronic fat diet–induced neuroinflammation.

Recent findings show a neuroprotective effect whereby RES reduces free radical formation in LPS-activated microglia of rats (39). Furthermore, RES has been shown to inhibit the production of nitric oxide and TNF-α by LPS-activated microglia (40). In addition, increased 4-HNE (a marker of lipid peroxidation) expression was found in the hippocampus after 20 weeks of HFD. Our results are in agreement with those finding that 4-HNE expression was increased in the cerebellum of HFD-fed rats (36). Oxidative stress in the brain coincided with hepatic steatosis, increased circulating levels of TNF-α, and increased hepatic 4-HNE in HFD-fed mice. Thus, our results indicate that HFD-induced peripheral inflammation and oxidative stress may be closely associated with neuroinflammation and lipid peroxidation during chronic diabetes, whereas dietary supplementation with RES can minimize these deleterious effects.

In general, insulin is synthesized by β-cells of the pancreatic islets of Langerhans and acts by reducing blood glucose levels in the periphery. In the CNS, insulin can be partially formed in the hippocampus, cortex, and olfactory bulb (41). Insulin in the CNS exerts its pleiotropic effects through binding to IRs and triggers the IR to undergo phosphorylation (42). There is evidence that insulin is capable of modulating of AMPK. As suggested by Tezapsidis et al. (43), we confirmed that activation of AMPK by IR leads to the phosphorylation of GSK-3β, which deactivates it and decreases the phosphorylation of tau (Fig. 6*G*).

Here, AMPK signaling–mediated systemic and brain metabolic dysfunction are associated with neurodegenerative diseases, such as AD. In our study, decreased adiponectin-mediated AMPK/ACC signaling in the hippocampus of HFD-fed mice was consistent with the reduction of renal adiponectin–mediated AMPK/ACC in STZ-induced diabetes (44). In agreement with results in peripheral organs, phosphorylation of AMPK was decreased in the hippocampus of rats fed the HFD (40%) compared with rats fed a regular diet (45). Hyperinsulinemia leads to a decrease in adiponectin concentrations in HFD-fed rats (46). Our current finding shows that decreased adiponectin expression in the hippocampus of HFD-fed mice is closely correlated with circulating levels of adiponectin. These data show that systemic and brain adiponectin levels may play an important role in the regulation of the AMPK/ACC signaling pathway. In addition, reduced levels of AMPK in our results may be a product of the high caloric content of the HFD that can lead to oxidative stress. However, our results showed that RES supplementation restored levels of AMPK and 4-HNE in the hippocampus. Adiponectin exhibits potent anti-inflammatory responses in vascular tissue in addition to its insulin-sensitizing effects in tissues involved in glucose and lipid metabolism (47). In endothelial cells, adiponectin suppresses the adverse effects of inflammatory cytokines and reduces the oxidative stress induced by oxidized LDL (48). Our results showed that hypoadiponectinemia and neuroinflammation are reversed by RES administration and improvement of diabetes. Thus, these findings suggest that inactivation of adiponectin-mediated AMPK signaling in the hippocampus of HFD-fed mice may contribute to brain energy dysregulation and neurodegeneration. Finally, this inactivation of AMPK may lead to activation of GSK-3β and increase phosphorylation of tau (Fig. 6*G*).

Impaired brain insulin signaling, which is causally linked to neurodegeneration, is helpful to understand the possible mechanisms of diabetes-induced AD. Using a mouse model of HFD-induced obesity, Moroz et al. (36) demonstrated that chronic HFD feeding of C57BL/6 mice induces mild neuropathological lesions but significant impairments in IR binding in the temporal lobe region. In accordance with mild neurodegeneration, although the phosphorylation of tau-protein was increased by HFD, we found no change in hippocampal A-β levels between LFD- and HFD-treated mice using ELISA, including Fluoro-Jade staining (data not shown). These data indicate that chronic HFD feeding for 20 weeks does not induce A-β–mediated neurodegeneration. On the other hand, the reduction of ChAT is correlated with pathological changes, whereas the increased activity of insulin improves the expression of ChAT (49). Recent findings show that insulin signaling may play an important role in the activities of cholinergic neurons through insulin-related proteins colocalized with ChAT (50). In the current study, we confirmed that RES inhibits down-regulation of HFD-induced ChAT expression and Golgi staining in the hippocampus. These results are consistent with the findings from the Morris water maze. Thus, our findings support the hypothesis that the impairment of insulin and adiponectin-mediated AMPK signaling in cholinergic neurons results in dysregulation of energy metabolism and impairs repair and cell survival.

In conclusion, our findings suggest that chronic dietary supplementation with RES may play an important role in reversing the deleterious actions of obesity on inflammation and memory in type 2 diabetic mice. Since obesity-induced insulin resistance also has been implicated in the progression of neurodegenerative diseases, natural compounds such as RES may have beneficial effects in retarding the progression of diabetes-induced neurodegenerative diseases.

ACKNOWLEDGMENTS

This research was supported by the Basic Science Research Program through the National Research Foundation of Korea funded by the Ministry of Education, Science, and Technology (No. 2011-0006196).

No potential conflicts of interest relevant to this article were reported.

B.T.J. and G.S.R. researched data, contributed to discussion, and wrote, reviewed, and edited the manuscript. E.A.J., H.J.S., and Y.L. researched data. D.H.L., H.J.K., S.S.K., G.J.C., and W.S.C. contributed to discussion and reviewed and edited the manuscript. G.S.R. is the guarantor of this work and, as such, had full access to all the data in the study and takes responsibility for the integrity of the data and the accuracy of the data analysis.

The authors thank Jeong Bin Kim for technical support.

REFERENCES

1. Muhammad S, Bierhaus A, Schwaninger M. Reactive oxygen species in diabetes-induced vascular damage, stroke, and Alzheimer's disease. J Alzheimers Dis 2009;16:775–785
2. Akomolafe A, Beiser A, Meigs JB, et al. Diabetes mellitus and risk of developing Alzheimer disease: results from the Framingham Study. Arch Neurol 2006;63:1551–1555
3. Hotamisligil GS, Shargill NS, Spiegelman BM. Adipose expression of tumor necrosis factor-alpha: direct role in obesity-linked insulin resistance. Science 1993;259:87–91
4. Xu H, Barnes GT, Yang Q, et al. Chronic inflammation in fat plays a crucial role in the development of obesity-related insulin resistance. J Clin Invest 2003;112:1821–1830
5. Weisberg SP, McCann D, Desai M, Rosenbaum M, Leibel RL, Ferrante AW Jr. Obesity is associated with macrophage accumulation in adipose tissue. J Clin Invest 2003;112:1796–1808
6. Zhao WQ, Alkon DL. Role of insulin and insulin receptor in learning and memory. Mol Cell Endocrinol 2001;177:125–134
7. de la Monte SM, Longato L, Tong M, Wands JR. Insulin resistance and neurodegeneration: roles of obesity, type 2 diabetes mellitus and non-alcoholic steatohepatitis. Curr Opin Investig Drugs 2009;10:1049–1060
8. Haan MN. Therapy insight: type 2 diabetes mellitus and the risk of late-onset Alzheimer's disease. Nat Clin Pract Neurol 2006;2:159–166
9. de la Monte SM, Wands JR. Review of insulin and insulin-like growth factor expression, signaling, and malfunction in the central nervous system: relevance to Alzheimer's disease. J Alzheimers Dis 2005;7:45–61
10. Schmatz R, Mazzanti CM, Spanevello R, et al. Resveratrol prevents memory deficits and the increase in acetylcholinesterase activity in streptozotocin-induced diabetic rats. Eur J Pharmacol 2009;610:42–48
11. Frémont L. Biological effects of resveratrol. Life Sci 2000;66:663–673
12. Kumar A, Sharma SS. NF-kappaB inhibitory action of resveratrol: a probable mechanism of neuroprotection in experimental diabetic neuropathy. Biochem Biophys Res Commun 2010;394:360–365
13. Giri S, Nath N, Smith B, Viollet B, Singh AK, Singh I. 5-aminoimidazole-4-carboxamide-1-beta-4-ribofuranoside inhibits proinflammatory response in glial cells: a possible role of AMP-activated protein kinase. J Neurosci 2004;24:479–487
14. Prasad R, Giri S, Nath N, Singh I, Singh AK. 5-aminoimidazole-4-carboxamide-1-beta-4-ribofuranoside attenuates experimental autoimmune encephalomyelitis via modulation of endothelial-monocyte interaction. J Neurosci Res 2006;84:614–625
15. Marambaud P, Zhao H, Davies P. Resveratrol promotes clearance of Alzheimer's disease amyloid-beta peptides. J Biol Chem 2005;280:37377–37382
16. Fullerton MD, Steinberg GR. SIRT1 takes a backseat to AMPK in the regulation of insulin sensitivity by resveratrol. Diabetes 2010;59:551–553
17. Long YC, Zierath JR. AMP-activated protein kinase signaling in metabolic regulation. J Clin Invest 2006;116:1776–1783
18. Shieh JM, Wu HT, Cheng KC, Cheng JT. Melatonin ameliorates high fat diet-induced diabetes and stimulates glycogen synthesis via a PKCzeta-Akt-GSK3beta pathway in hepatic cells. J Pineal Res 2009;47:339–344
19. Towler MC, Hardie DG. AMP-activated protein kinase in metabolic control and insulin signaling. Circ Res 2007;100:328–341
20. Greco SJ, Sarkar S, Johnston JM, Tezapsidis N. Leptin regulates tau phosphorylation and amyloid through AMPK in neuronal cells. Biochem Biophys Res Commun 2009;380:98–104
21. Takeda S, Sato N, Uchio-Yamada K, et al. Diabetes-accelerated memory dysfunction via cerebrovascular inflammation and Abeta deposition in an Alzheimer mouse model with diabetes. Proc Natl Acad Sci U S A 2010;107:7036–7041
22. den Boer M, Voshol PJ, Kuipers F, Havekes LM, Romijn JA. Hepatic steatosis: a mediator of the metabolic syndrome. Lessons from animal models. Arterioscler Thromb Vasc Biol 2004;24:644–649
23. Whitmer RA, Gustafson DR, Barrett-Connor E, Haan MN, Gunderson EP, Yaffe K. Central obesity and increased risk of dementia more than three decades later. Neurology 2008;71:1057–1064
24. Terry RD, Davies P. Dementia of the Alzheimer type. Annu Rev Neurosci 1980;3:77–95
25. Moreira PI, Duarte AI, Santos MS, Rego AC, Oliveira CR. An integrative view of the role of oxidative stress, mitochondria and insulin in Alzheimer's disease. J Alzheimers Dis 2009;16:741–761
26. Milatovic D, Montine TJ, Zaja-Milatovic S, Madison JL, Bowman AB, Aschner M. Morphometric analysis in neurodegenerative disorders. Curr Protoc Toxicol 2010 Feb;Chapter 12:Unit 12.16
27. Gasparini L, Netzer WJ, Greengard P, Xu H. Does insulin dysfunction play a role in Alzheimer's disease? Trends Pharmacol Sci 2002;23:288–293
28. Godbout JP, Chen J, Abraham J, et al. Exaggerated neuroinflammation and sickness behavior in aged mice following activation of the peripheral innate immune system. FASEB J 2005;19:1329–1331
29. Sun AY, Simonyi A, Sun GY. The "French Paradox" and beyond: neuroprotective effects of polyphenols. Free Radic Biol Med 2002;32:314–318
30. Baur JA, Pearson KJ, Price NL, et al. Resveratrol improves health and survival of mice on a high-calorie diet. Nature 2006;444:337–342
31. Lagouge M, Argmann C, Gerhart-Hines Z, et al. Resveratrol improves mitochondrial function and protects against metabolic disease by activating SIRT1 and PGC-1alpha. Cell 2006;127:1109–1122
32. Um JH, Park SJ, Kang H, et al. AMP-activated protein kinase-deficient mice are resistant to the metabolic effects of resveratrol. Diabetes 2010;59:554–563
33. Lumeng CN, Deyoung SM, Bodzin JL, Saltiel AR. Increased inflammatory properties of adipose tissue macrophages recruited during diet-induced obesity. Diabetes 2007;56:16–23
34. Buettner R, Schölmerich J, Bollheimer LC. High-fat diets: modeling the metabolic disorders of human obesity in rodents. Obesity (Silver Spring) 2007;15:798–808
35. Wellen KE, Hotamisligil GS. Inflammation, stress, and diabetes. J Clin Invest 2005;115:1111–1119
36. Moroz N, Tong M, Longato L, Xu H, de la Monte SM. Limited Alzheimer-type neurodegeneration in experimental obesity and type 2 diabetes mellitus. J Alzheimers Dis 2008;15:29–44
37. De Souza CT, Araujo EP, Bordin S, et al. Consumption of a fat-rich diet activates a proinflammatory response and induces insulin resistance in the hypothalamus. Endocrinology 2005;146:4192–4199
38. Sheng JG, Zhou XQ, Mrak RE, Griffin WS. Progressive neuronal injury associated with amyloid plaque formation in Alzheimer disease. J Neuropathol Exp Neurol 1998;57:714–717
39. Candelario-Jalil E, de Oliveira AC, Gräf S, et al. Resveratrol potently reduces prostaglandin E2 production and free radical formation in lipopolysaccharide-activated primary rat microglia. J Neuroinflammation 2007;4:25
40. Meng XL, Yang JY, Chen GL, et al. RV09, a novel resveratrol analogue, inhibits NO and TNF-alpha production by LPS-activated microglia. Int Immunopharmacol 2008;8:1074–1082
41. Baskin DG, Figlewicz DP, Woods SC, Porte D Jr, Dorsa DM. Insulin in the brain. Annu Rev Physiol 1987;49:335–347
42. Kasuga M, Zick Y, Blith DL, Karlsson FA, Häring HU, Kahn CR. Insulin stimulation of phosphorylation of the beta subunit of the insulin receptor. Formation of both phosphoserine and phosphotyrosine. J Biol Chem 1982;257:9891–9894
43. Tezapsidis N, Johnston JM, Smith MA, et al. Leptin: a novel therapeutic strategy for Alzheimer's disease. J Alzheimers Dis 2009;16:731–740
44. Guo Z, Zhao Z. Effect of N-acetylcysteine on plasma adiponectin and renal adiponectin receptors in streptozotocin-induced diabetic rats. Eur J Pharmacol 2007;558:208–213
45. Wu A, Ying Z, Gomez-Pinilla F. Oxidative stress modulates Sir2alpha in rat hippocampus and cerebral cortex. Eur J Neurosci 2006;23:2573–2580
46. Li L, Yang G, Li Q, Tang Y, Li K. High-fat- and lipid-induced insulin resistance in rats: the comparison of glucose metabolism, plasma resistin and adiponectin levels. Ann Nutr Metab 2006;50:499–505
47. Trujillo ME, Scherer PE. Adiponectin—journey from an adipocyte secretory protein to biomarker of the metabolic syndrome. J Intern Med 2005;257:167–175
48. Motoshima H, Wu X, Mahadev K, Goldstein BJ. Adiponectin suppresses proliferation and superoxide generation and enhances eNOS activity in endothelial cells treated with oxidized LDL. Biochem Biophys Res Commun 2004;315:264–271
49. Rivera EJ, Goldin A, Fulmer N, Tavares R, Wands JR, de la Monte SM. Insulin and insulin-like growth factor expression and function deteriorate with progression of Alzheimer's disease: link to brain reductions in acetylcholine. J Alzheimers Dis 2005;8:247–268
50. Wang H, Wang R, Zhao Z, et al. Coexistences of insulin signaling-related proteins and choline acetyltransferase in neurons. Brain Res 2009;1249:237–243